Cancer Management and Research

Dovepress

open access to scientific and medical research

Open Access Full Text Article

ORIGINAL RESEARCH

LncRNA PROX1-AS1 Facilitates Gastric Cancer Progression via miR-877-5p/PD-L1 Axis

This article was published in the following Dove Press journal:
Cancer Management and Research

TianWei Guo[1,*]
Wei Wang[2,*]
YueXia Ji[1]
Min Zhang[3]
GuoYing Xu[4]
Sen Lin[5]

[1]Department of Pathology, Changshu Hospital Affiliated to Nanjing University of Chinese Medicine, Changshu, Jiangsu, People's Republic of China; [2]Department of Pathology, The Affiliated Obstetrics and Gynecology Hospital of Nanjing Medical University, Nanjing Maternity and Child Health Care Hospital, Nanjing, Jiangsu, People's Republic of China; [3]Department of Pathology, Children's Hospital Affiliated to Soochow University, Suzhou, Jiangsu, People's Republic of China; [4]School of Medical Technology, Jiangsu College of Nursing, Huai'an, Jiangsu, People's Republic of China; [5]The Affiliated Huai'an Hospital of Xuzhou Medical University and the Second People's Hospital of Huai'an, Huai'an, Jiangsu, People's Republic of China

*These authors contributed equally to this work

Correspondence: Sen Lin
The Affiliated Huai'an Hospital of Xuzhou Medical University and the Second People's Hospital of Huai'an, Huai'an, Jiangsu, People's Republic of China
Email linsen378@163.com

GuoYing Xu
School of Medical Technology, Jiangsu College of Nursing, Huai'an, Jiangsu, People's Republic of China
Email xuguoying3@163.com

Introduction: Growing evidences imply that multiple long non-coding RNAs (lncRNAs) play a significant role in the treatment of cancer. Therefore, it is of great significance to discover new biomarkers or therapeutic targets of gastric cancer (GC). However, the potential molecular mechanism of lncPROX1-AS1 in GC remains unknown. The objective of current study is to investigate the effect of PROX1-AS1 in GC.

Methods: Thus, we detect that PROX1-AS1 is over-expressed in tissues and cell lines of GC using qRT-PCR analysis. CCK-8, colony formation, flow cytometry, wounding healing and transwell analyses were performed to explore the effect of PROX1-AS1 on GC malignant behaviors.

Results: It is further disclosed that silencing of PROX1-AS1 represses cell proliferation, migration, and invasion, whereas promotes cell apoptosis in GC. Bioinformatics analysis suggests that miR-877-5p is negatively regulated by PROX1-AS1 and ectopic of miR-877-5p alleviates the malignant behaviors of GC. Subsequently, miR-877-5p suppresses the activity of PD-L1-3′ UTR. At last, rescue assays demonstrated that the GC progression is suppressed by sh-PROX1-AS1 and facilitated on account of miR-877-5p inhibitors and then is retrieved by sh-PD-L1.

Discussion: Our findings reveal that PROX1-AS1 exerts its role via miR-877-5p/PD-L1 axis in the GC progression, suggesting that PROX1-AS1 may represent a new therapeutic target for the diagnosis and treatment of GC patients.

Keywords: PROX1-AS1, miR-877-5p, PD-L1, proliferation, apoptosis, gastric cancer

Introduction

As one of the most common malignant tumors with high mortality and high incidence rate worldwide,[1,2] the morbidity of gastric cancer (GC) has increased steadily over the past decade.[3–5] Despite significant advancements in diagnosis and surgical treatment, most patients have already stepped into progressive stage upon definite diagnosis and the survival rate of GC remains low.[6,7] Additionally, the underlying molecular mechanism in the process of GC remains elusive. Therefore, it is urgent to deeply understand the potential mechanism from the genetic and molecular level of GC.[8]

Long non-coding RNAs (lncRNAs) are non-coding RNA sequences with more than 200nt in length. Previous reports have proved that lncRNAs function as crucial regulators in tumor progression, including GC.[9–13] In papillary thyroid cancer, lncRNA GAS8-AS1 suppresses cell proliferation by regulating ATG5.[14] Moreover, knockdown of lncRNA UCA1 inhibits cervical cancer cell proliferation and invasion through targeting miR-206.[15] PROX1 antisense RNA 1 (PROX1-AS1) is transcribed

submit your manuscript | www.dovepress.com
DovePress
http://doi.org/10.2147/CMAR.S275352

from the antisense strand of PROX1 and a large body of evidence indicates that PROX1-AS1 is generally up-regulated and exerts its carcinogenic activity in many cancers. However, the potential function of PROX1-AS1 /miR-877-5p/PD-L1 in GC remained obscure.

All these findings suggested that PROX1-AS1 might have therapeutic effects on tumor progression. Thus, the objective of our study was to explore the biological function and underlying mechanisms of PROX1-AS1 which interacted with miR-877-5p and PD-L1 in GC. Our study might provide evidence that PROX1-AS1 functioned as a useful target for the GC patient treatment.

Materials and Methods

Clinic Samples

Freshly dissected GC tissues and paired adjacent normal tissues from 30 patients in the Changshu Hospital Affiliated to Nanjing University of Chinese Medicine. Certainly, these patients had signed informed consent. Our project was approved by Research Ethics Committee of the Changshu Hospital Affiliated to Nanjing University of Chinese Medicine (No: 201901026). The clinic information of patients are shown in Table 1 and we tested the expression level of PROX1-AS1 in patient samples and select the median as the classification standard, low expression for those lower than the median, high expression for those higher than the median.

Table 1 Association of PROX1-AS1 Expression with Clinic-Pathological Features of GC Patients

Characteristics	Number	Low (n=15)	High (n=15)	P value
Sex				0.51
Male	17	9	8	
Female	13	6	7	
Age				0.36
≤60	17	10	7	
>60	13	5	8	
Tumor size, cm				0.032
≤4	18	11	7	
>4	12	4	8	
Pathological Staging				0.0452
I + II	16	11	5	
III + IV	14	4	10	
Metastasis				0.0247
Yes	16	5	11	
No	14	10	4	

Cell Lines and Cell Culture

Four GC cell lines (AGS, MGC-803, SGC-7901, SNU-1) and normal epithelial cell lines GES-1were purchased from ATCC (USA). GES-1 cells were maintained in DMEM medium (Gibco, USA) and AGS, MGC-803, SGC-7901 and SNU-1 cells were cultured in RPMI-1640 medium (Life Technologies, USA) supplemented with 10% fetal bovine serum (FBS; Gibco, USA) and cultured at 37°C in a humidified atmosphere comprising 5% CO_2.

Quantitative Real-Time PCR (qRT-PCR) Analysis

TRIzol reagent (Takara, Japan) was applied to collect the total RNA from tissues and cells. A PrimeScript RT reagent kit (Takara, Japan) was used to reverse-transcribed RNA into cDNA. qRT-PCR was carried out by SYBR premix Ex Taq reagent kit (Takara, Japan) and miRNA was detected by a miRcute miRNA qPCR kit (TIANGEN, China) running by fluorescent quantitative PCR 7500 (ABI, USA). GAPDH and U6 were used as the internal reference. $2^{-\Delta\Delta Cq}$ method was used to calculate the fold changes of gene expression and the experiment was conducted three times.

Western Blot Analysis

The total proteins were extracted and separated using SDS-PAGE, and then transferred into the polyvinylidene fluoride (PVDF) membranes. The membranes were incubated by the primary antibodies at 4°C overnight after being blocked by skimmed milk, and probed with the secondary horseradish peroxidase (HRP) antibodies (Sigma, Aldrich) for 1 h. The primary antibodies listed as followed: cyclin D1 (ab40754, 1:1000), p21 (ab80633, 1:1000), Bax (ab53154, 1:1000), Bcl-2 (ab196495, 1:1000), cleaved caspase-3 (ab49822, 1:1000), cleaved caspase-9 (ab2324, 1:1000), Cox-2 (ab62331, 1:1000), MMP-2 (ab86607, 1:1000), MMP-9 (ab38898, 1:1000), PD-L1 (AB213524, 1:1000) and GAPDH (ab9435, 1:1000). The antibodies were purchased from Abcam company. The protein bands were visualized by using Image J 6.0 software (Rockville, MD).

Cell Transfection

AGS and SGC7901 cells (1×10^5) were seeded into 6 well plates and cultured reaching to 60%-70% confluence, siRNAs against PROX1-AS1 (sh-PROX1-AS1), sh-NC,

miR-877-5p mimic, NC mimic, inhibitor, NC inhibitor or sh-PD-L1 were transfected into AGS and SGC7901 cells using Lipofectamine 2000 (Invitrogen, USA). Transfected cells were subjected to RT-qPCR assay to assess the transfection efficacy.

Cell Counting Kit-8 (CCK-8) Assay

Cells (1×10^5) were seeded into 96-well plates and harvested. Then, 10 mL CCK-8 reagent (Gibco, USA) was added and cells were subsequently maintained for (24 h, 48 h, 72 h and 96 h). The optical density (OD) was tested at 450 nm using a microplate reader (BMG Labtech, Germany). These tests were carried out in triplicate.

Colony Formation Analysis

Colony formation analysis was carried out to investigate the function of PROX1-AS1 on the proliferation of AGS and SGC7901 cells. In brief, 1×10^5 transfected cells were maintained and grew in DMEM medium containing 10% FBS. Fourteen days later, the medium was discarded and then cells were fixed in 4% paraformaldehyde after being stained with crystal violet for 30 min. Colonies were counted and photographed under a light microscope.

Flow Cytometry Analysis

Centrifuged at 1500 rpm for 10 min after a 48-h transfection, the cells (1×10^5) were trypsinized and dispersed into cell suspension. Then the cells were fixed with 70% ethanol at 4°C overnight. For cell cycle analysis, cell suspension was stained with 50 mg of 1% propidium iodide (PI) containing RNAase for 30 min, and was detected on a flow cytometer (BD Biosciences, Franklin Lakes, USA). For cell apoptosis analysis, an annexin V-fluorescein isothiocyanate (FITC)/PI reagent kit (Beyotime, China) was utilized. FITC was tested using a flow cytometer (Cube 6, Partec, Germany) at wavelength of 480 and 530 nm and PI determined at wavelength of 575 nm. The data were analyzed by FlowJo v10 software (Tree Star, Inc.).

Wound Healing Assay

AGS and SGC7901 cells were seeded in plates and cells grew to approximately 90% confluence, followed by scratching with a 10 μL pipette tip. The migrated cells were photographed at 0 h and 48 h under a light microscope.

Transwell Chamber Assay

Transwell chamber assay was applied to assess the cell migration and invasion abilities. Cells were plated in 24-well upper uncoated chambers (BD Biosciences, CA, USA) with serum-free medium for migration analysis and the upper chamber loaded with matrigel for invasion analysis. Culture medium was filled in the lower chamber to culture for 48 h. Then the cells which did not migrated and invaded to the lower chamber were removed. Cells were fixed stained with crystal violet. Finally, the number of cells were counted under a light microscope (×200 magnification) in five random fields.

Fractionation of Nuclear and Cytoplasmic RNA

The PROX1-AS1 nucleus fraction and cytoplasmic fraction of PROX1-AS1 were extract using Cytoplasmic and Nuclear RNA Purification Kit (Norgen, Belmont, CA, USA) according to the manufacturer's protocol.

Dual-Luciferase Reporter Assay

We predicted the PROX1-AS1 binding sites of miR-877-5p and the miR-877-5p binding sites of PD-L1 with bioinformatics tools. AGS and SGC7901 cells were transfected with 150 ng of empty pmirGLO-NC, pmirGLO-PROX1-AS1-WT or Mut. 2 ng of pRL-TK (Promega, WI, USA) and miR-877-5p mimics or NC mimics were co-transfected into AGS and SGC7901 cells using Lipofectamine 2000 (Invitrogen, USA). The relative luciferase activity was assessed after 48-h transfection. The principle was the same as above when verifying the targeting relationship between miR-877-5p and PD-L1. The data of these experiments were analyzed by FlowJo v10 software (Tree Star, Inc.).

Statistical Analysis

All of our tests were conducted for three times and the data were presented as the mean ± SD. Statistical analyses were performed using SPSS v19.0 software (IBM Corp.). Student's *t*-test was carried out to evaluate significant differences between two groups of samples. The differences among multiple groups were analyzed using One-way ANOVA, followed by Tukey's post hoc test. $P < 0.05$ was considered as a significant difference.

Results

PROX1-AS1 Expression is Up-Regulated and Positively Correlates with Poor Prognosis in GC

The PROX1-AS1 expression pattern was determined in 30 GC tissues through RT-qPCR assay. The result had shown that PROX1-AS1 expression pattern was dramatically over-expressed in GC tissues compared to normal tissues (mean ratio of 1.9-fold, $P < 0.05$) (Figure 1A). Furthermore, we explored the correlation between PROX1-AS1 expression and clinical pathological features. As shown in Figure 1B, PROX1-AS1 up-regulation correlated with advanced pathological stage (III+IV; n=15) compared to I+II stage (n=15) ($P < 0.05$). Next, we analyzed whether PROX1-AS1 expression was associated with overall survival rate using the Kaplan-Meier method, and proved that PROX1-AS1 expression was relative to patient survival rate. In addition, patients with high PROX1-AS1 expression had a markedly poorer prognosis than those with low PROX1-AS1 expression (Figure 1C). Additionally, the expression pattern of PROX1-AS1 in GC cells was investigated. We observed that the abundance of PROX1-AS1 in AGS, MGC-803, SGC-7901, SNU-1 cells were notably higher than that in normal epithelial cells (GES-1) (Figure 1D; $P < 0.01$). Our findings implied that PROX1-AS1 might be a vital biomarker in the progression of GC.

PROX1-AS1 Knockdown Suppresses the Proliferation and Enhances Apoptosis of GC Cells

We firstly investigated whether PROX1-AS1 affected cell proliferation of GC cells so as to identify the function of PROX1-AS1 in GC. Considering that PROX1-AS1 expression in AGS and SGC7901 was higher than that in other GC cell lines, AGS and SGC7901 cells were selected for further assessment.

Thus, loss-of-function strategies were applied to explore the biological role of PROX1-AS1 in GC cells. Sh-NC and sh-PROX1-AS1 were transfected into AGS and SGC7901 cells. Next, the transfection efficiency was verified by RT-qPCR analysis. As shown in Figure 2A, sh-PROX1-AS1 obviously down-regulated the expression level of PROX1-AS1 compared to the sh-NC group ($P < 0.01$). Next, CCK-8 assay found that sh-PROX1-AS1 reduced the cell viability compared with sh-NC group (Figure 2B; $P < 0.05$). Similarly,

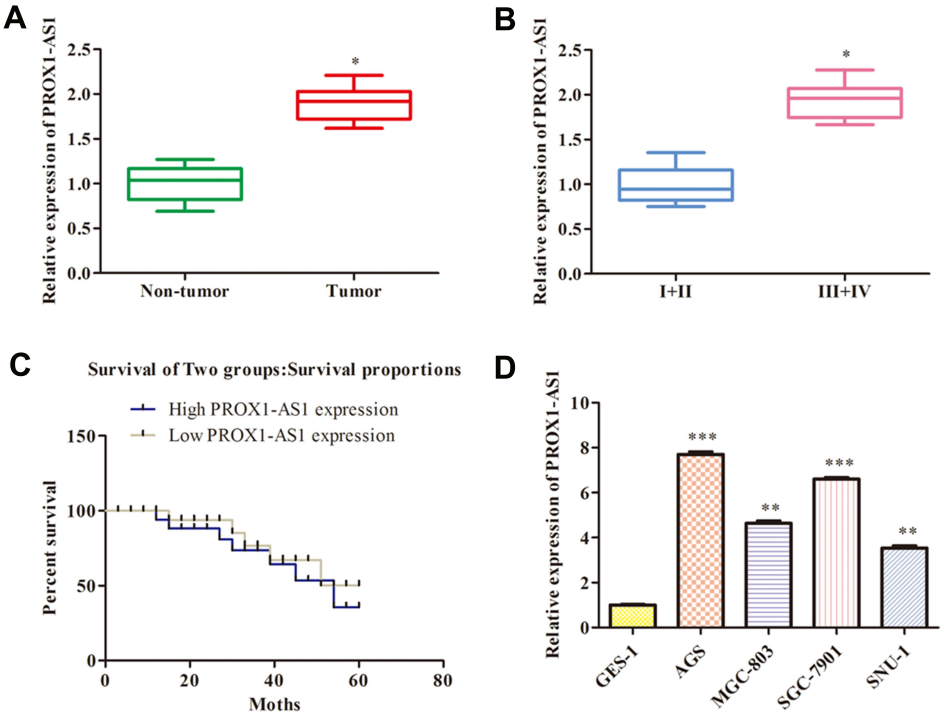

Figure 1 PROX1-AS1 expression is up-regulated in GC and positively correlates with poor prognosis. (**A**) The PROX1-AS1 mRNA level in GC tissues and the corresponding normal tissues were detected by RT-qPCR assay. (**B**) Examination of the correlation between PROX1-AS1 expression and clinical pathological features showed that PROX1-AS1 up-regulation correlated with advanced pathological stage. (**C**) Kaplan-Meier curves for overall survival analysis based on PROX1-AS1 expression. (**D**) The expression of PROX1-AS1 was assessed in GC cells. *P < 0.05, **P < 0.01, ***P < 0.001 vs Non-tumor, I+II or GES-1 group.

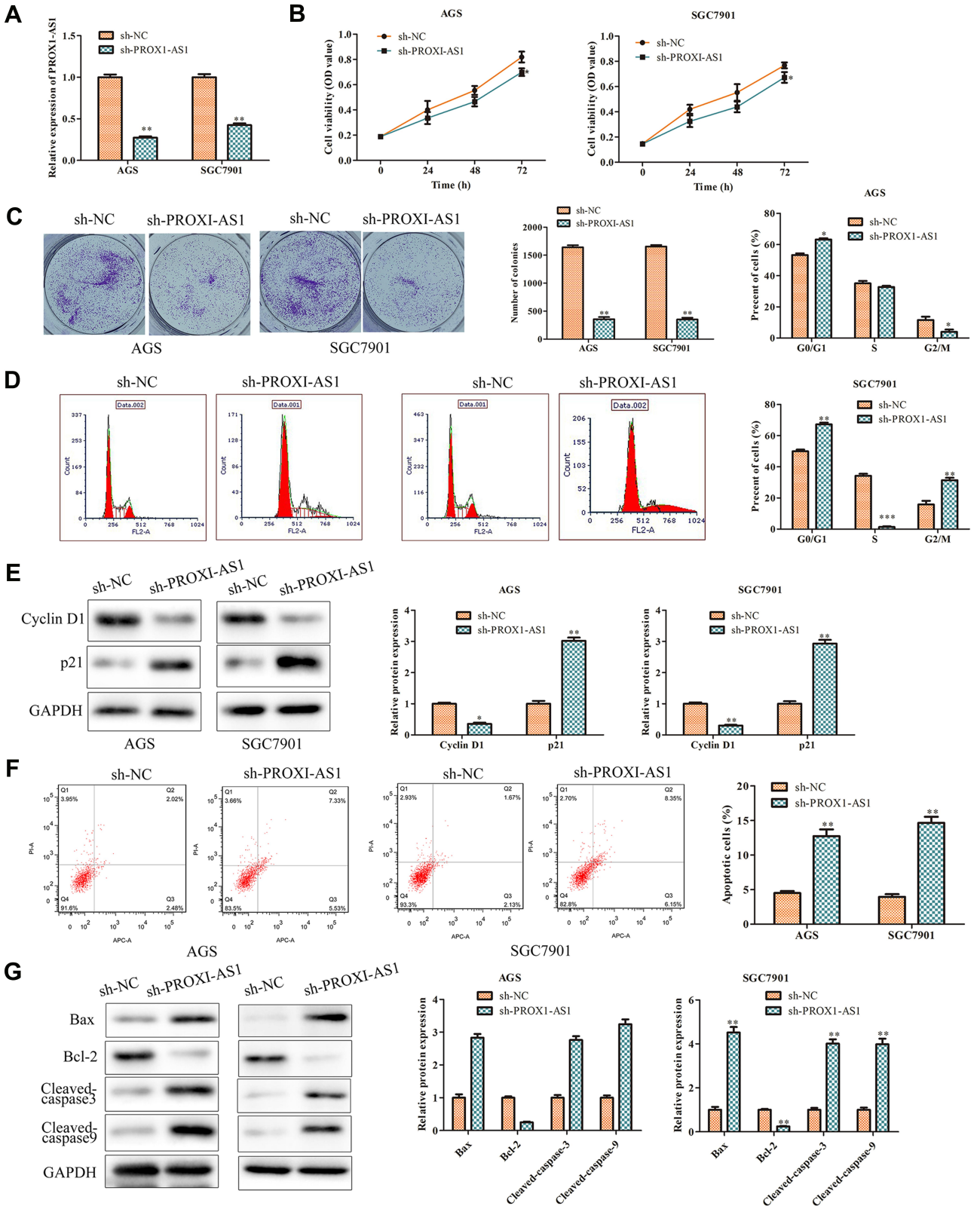

Figure 2 PROX1-AS1 knockdown suppresses the proliferation and promotes apoptosis of GC cells. (**A**) Transfection efficiency was verified by RT-qPCR analysis. (**B**) Cell viability was examined by CCK-8 assay. (**C**) The functional role of PROX1-AS1 on colony formation was analyzed by colony formation assay (magnification, 40×). (**D**) Cell cycle was assessed by flow cytometry assay. (**E**) The expression of cell cycle regulatory proteins was analyzed using Western blot. (**F**) Cell apoptosis was assessed by flow cytometry assay. (**G**) The expression of cell apoptosis regulatory proteins was analyzed using Western blot. *P < 0.05, **P < 0.01, ***P < 0.001 vs sh-NC group.

colony formation assay also indicated that congenic survival was reduced following inhibition of PROX1-AS1 in AGS and SGC7901 cells (Figure 2C; $P < 0.01$). Next, we performed the flow cytometry and Western blot assays to explore the role of PROX1-AS1 on cell cycle and apoptosis. Following the inhibition of PROX1-AS1, the proportion of AGS and SGC7901 cells at the G0/G1 phase were increased, while the proportion at the S phase was reduced, indicating that PROX1-AS1 served as an inhibitor of cell cycle progression (Figure 2D; $P < 0.05$). In addition, the results of Figure 2E suggested that knockdown of PROX1-AS1 repressed the expression levels of cyclin D1, while enhancing the level of p21 compared with sh-NC group ($P < 0.01$). Additionally, cell apoptotic rate was markedly increased in cells which were transfected with sh-PROX1-AS1 (Figure 2F; $P < 0.01$). The data of Western blot analysis indicated that knockdown of PROX1-AS1 increased Bax, cleaved-caspase-3 and cleaved-caspase-9 levels, while decreasing Bcl-2 levels (Figure 2G; $P < 0.01$). These results indicated that knockdown of PROX1-AS1 suppressed proliferation and enhanced apoptosis of GC cells.

Inhibition of PROX1-AS1 Suppresses the Migration and Invasion of GC Cells

It was generally known that cell migration and invasion was a significant aspect of cancer progression. Hence, we conducted wound healing assay to estimate whether PROX1-AS1 affected the mobility of AGS and SGC7901 cells. Transfection of sh-PROX1-AS1 impeded the migration ability of AGS (37.4%) and SGC7901 (40.6%) cells compared with sh-NC group (Figure 3A; $P < 0.01$). Moreover, we performed transwell assay to explore the cell invasion ability. The result of Figure 3B indicated that knockdown of PROX1-AS1 significantly suppressed invasion capacity of AGS and SGC7901 cells ($P < 0.01$). Moreover, Western blot analysis indicated that sh-PROX1-AS1 repressed the migration- and invasion-associated protein expressions (MMP-2, MMP-9) both in AGS and SGC7901 cells (Figure 3C; $P < 0.01$). Therefore,

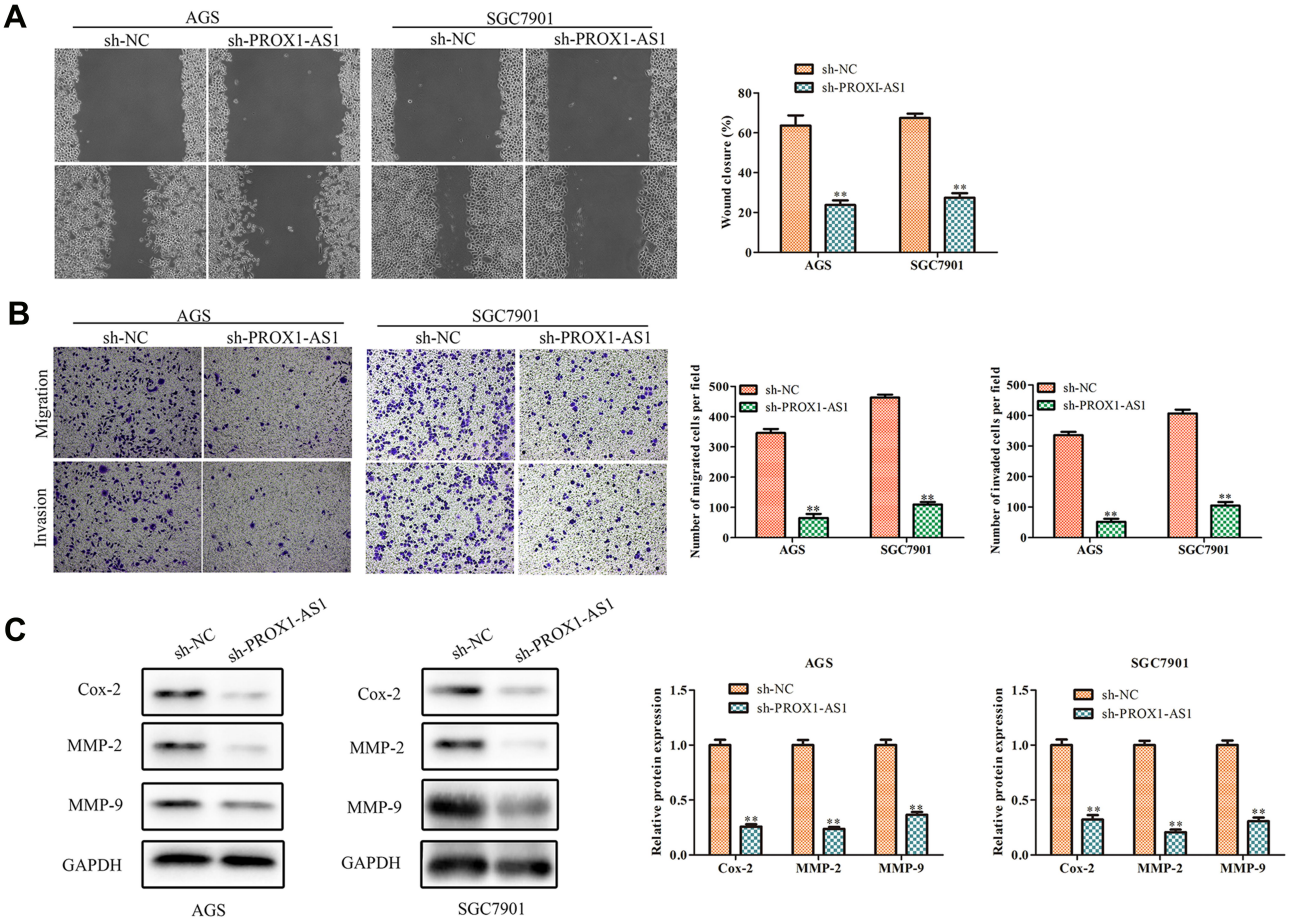

Figure 3 Inhibition of PROX1-AS1 suppresses the migration and invasion of GC cells. (**A**, **B**) The wound-healing assay and transwell chamber assays were used to assess cell migration and invasion. (**C**) The protein expression levels of MMP-2 and MMP-9 in AGS and SGC7901 cells. **P < 0.01 vs sh-NC group.

our study suggested that PROX1-AS1 knockdown exerted suppressive impacts on GC cell migration and invasion.

PROX1-AS1 Serves as a Molecular Sponge for miR-877-5p

Subcellular fractionation analysis indicated that PROX1-AS1 was markedly located in the cytoplasm both in AGS and SGC7901 cells, suggesting that PROX1-AS1 might serve as a competitive endogenous RNA (ceRNA) in GC (Figure 4A; $P < 0.01$). To elucidate the molecular mechanism of PROX1-AS1 in regulating the progression of GC, StarBase v2.0 (http://starbase.sysu.edu.cn/) was applied to predict the potential target of PROX1-AS1. Among all the targets, miR-877-5p was chosen for further study, since functions as an important regulator controlling the occurrence and development of various tumors, including GC.[16–18] The binding site between PROX1-AS1 and miR-877-5p are as shown in Figure 4B. Moreover, the result of luciferase reporter analysis indicated that the luciferase activity was suppressed in miR-877-5p mimic of wild-type PROX1-AS1 group but did not affect the mutant group (Figure 4C; $P < 0.01$). RT-qPCR results delineated that sh-PROX1-AS1 increased miR-877-5p expression levels (Figure 4D). In addition, miR-877-5p expression in GC tissues was assessed and found that miR-877-5p was lower than that in normal tissues (Figure 4E; $P < 0.05$). Further, we explored miR-877-5p expression in GC cell lines and same result was obtained (Figure 4F; $P < 0.01$). In concert with the above results, Pearson's correlation analysis unveiled the negative relevance between PROX1-AS1 and miR-877-5p (Figure 4G).

Over-Expressed miR-877-5p Inhibits GC Progression

RT-qPCR assay was adopted to verify the transfection efficiency of miR-877-5p mimic and the results are

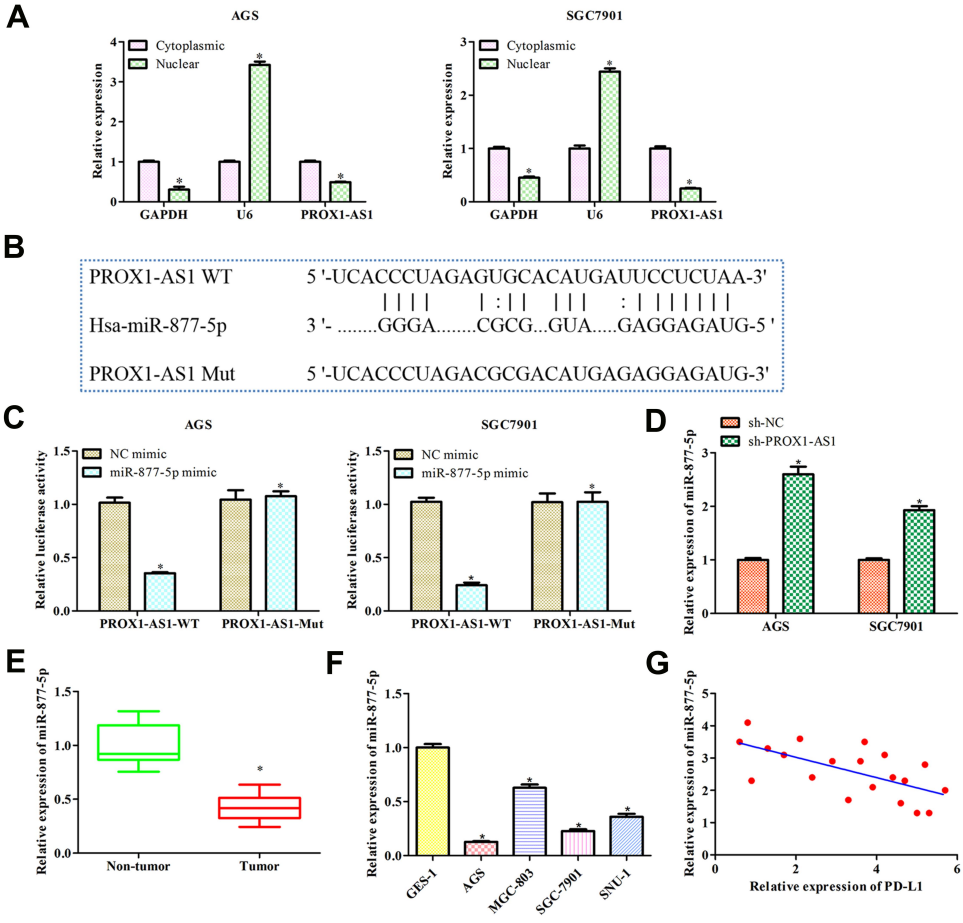

Figure 4 PROX1-AS1 acts as a molecular sponge for miR-877-5p. (**A**) The subcellular location analysis of PROX1-AS1. (**B**) Putative binding regions of PROX1-AS1 in miR-877-5p predicted by StarBase. (**C**) Luciferase reporter assay was conducted to verify the relationship between PROX1-AS1 and miR-877-5p. (**D**) RT-qPCR was used to detect miR-877-5p expression level after sh-PROX1-AS1 treatments. (**E**, **F**) The mRNA expression of miR-877-5p in GC tissues and cell lines were analyzed by RT-qPCR. (**G**) Pearson's correlation analysis between PROX1-AS1 and miR-877-5p expression. *$P < 0.05$ vs Cytoplasmic, NC mimics, Non-tumor, or GES-1 group.

shown in Figure 5A. Then, CCK-8 and colony formation analyses were performed to explore the effect of miR-877-5p on GC. The data demonstrated that ectopic of miR-877-5p suppressed the proliferation ability of AGS and SGC7901 cells when accompanying with the cells transfected with NC mimic (Figure 5B, C; $P < 0.01$). The roles of miR-877-5p on cell apoptosis were verified by flow cytometry assay. As shown in Figure 5D, cell apoptotic rate was markedly increased in cells transfected with miR-877-5p mimic ($P < 0.01$). Additionally, we found that miR-877-5p mimic notably decreased the migration and invasion capabilities compared with NC mimic group both in AGS and SGC7901 cells by transwell assay (Figure 5E; $P < 0.01$).

PD-L1 is Target Gene of miR-877-5p

Bioinformatic analysis was used in our study to search for genes that were directly regulated by miR-877-5p. We found that PD-L1 was the putative target of miR-877-5p (http://starbase.sysu.edu.cn/) (Figure 6A) and down-regulation of PD-L1 that plays suppressive effects in GC cells is well known.[19,20] Data of Figure 6B declared that miR-877-5p mimic remarkably suppressed luciferase activity of PD-L1 3′ UTR wild type, while not affecting the activity of mutant form through luciferase reporter assay ($P < 0.01$). The levels of PD-L1 in miR-877-5p mimic and NC mimic group were determined using RT-qPCR and Western blot analyses. Results showed that PD-L1 was decreased while miR-877-5p overexpressed (Figure 6C and D; $P < 0.01$). In addition, PD-L1 was

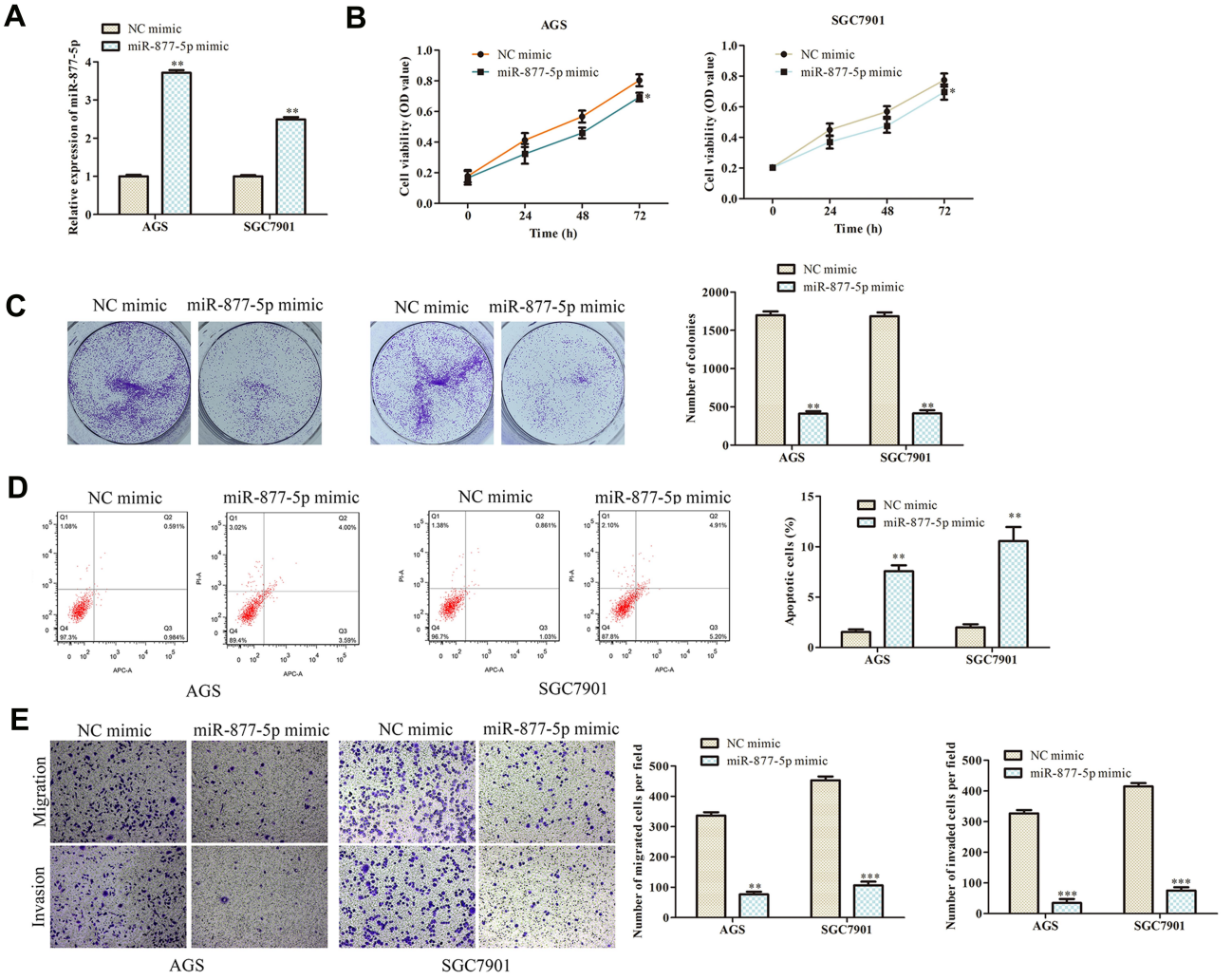

Figure 5 Overexpression of miR-877-5p inhibits GC progression. (**A**) RT-qPCR was used to detect the transfection efficiency of miR-877-5p mimic. (**B**) Cell viability was examined by CCK-8 assay. (**C**) The functional role of miR-1303 on colony formation was analyzed by colony formation assay (magnification, 40×). (**D**) Cell apoptosis was assessed by flow cytometry assay. (**E**) The effects of miR-877-5p on cell migration and invasion were measured by transwell assay (magnification, 200×). *$P < 0.05$, **$P < 0.01$, ***$P < 0.001$ vs NC mimic group.

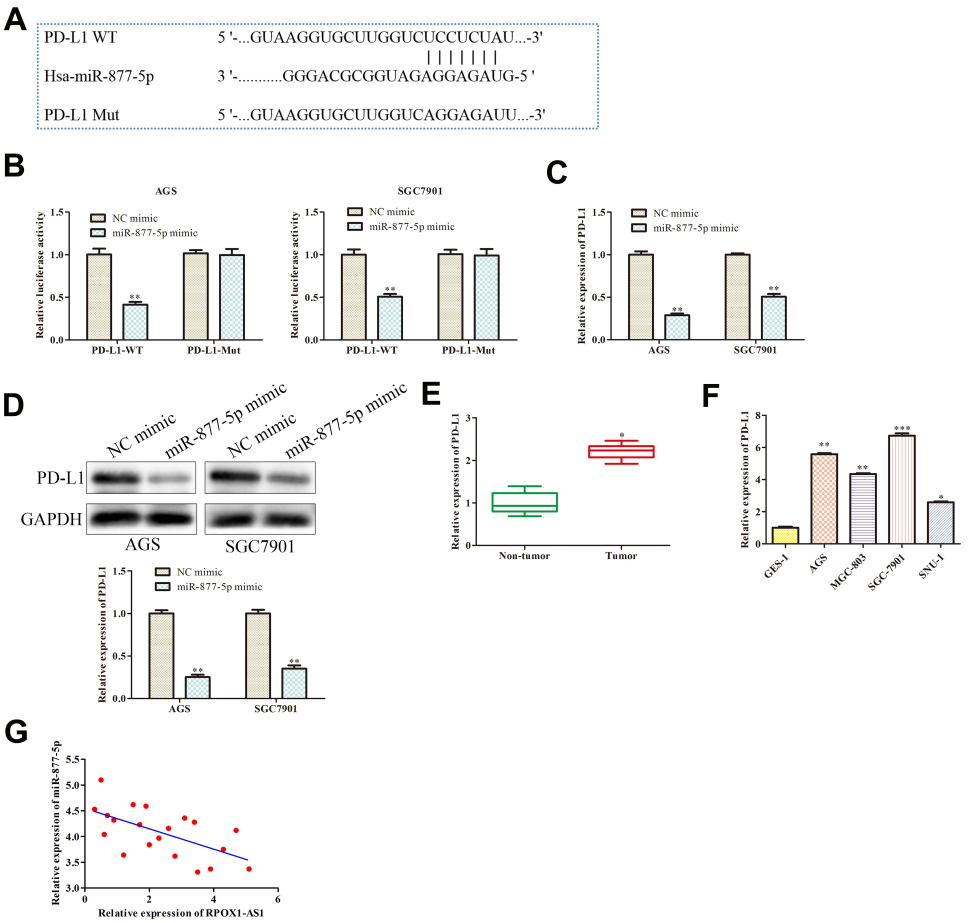

Figure 6 PD-L1 is target gene of miR-877-5p. (**A**) The predicted binding site of miR-877-5p in the 3′-UTR of PD-L1. (**B**) The relative luciferase activity was detected. (**C**, **D**) Relative expression of PD-L1 was examined by RT-qPCR and Western blot assay. **P < 0.01 vs NC mimic. (**E**, **F**) The mRNA expression of PD-L1 in GC tissues and cell lines were analyzed by RT-qPCR. (**G**) Pearson's correlation analysis between miR-877-5p and PD-L1 expression. *P < 0.05, **P < 0.01, ***P < 0.001 vs NC mimics, Non-tumor, or GES-1 group.

demonstrated to be up-regulated in GC tissues and cell lines (Figure 6E and F; $P < 0.05$). Moreover, Pearson's correlation analysis unveiled the negative relevance between miR-877-5p and PD-L1 expression levels in GC (Figure 6G).

PROX1-AS1 Accelerates Cell Growth, Invasion and Suppresses Apoptosis by Targeting miR-877-5p/PD-L1 Axis

Rescue assays were performed to further study whether PROX1-AS1 executed its function in GC via miR-877-5p/PD-L1 axis. As presented in Figure 7A, the transfection efficiencies of miR-877-5p inhibitor or sh-PD-L1 were measured. Functionally, CCK-8 and colony formation analyses were applied to detect the proliferation ability of AGS and SGC7901 cells. We found that the repression role of sh-PROX1-AS1 on cell proliferation was aggravated by miR-877-5p inhibitor and then retrieved when PD-L1 was silenced (Figure 7B, C; $P < 0.01$). On the contrary, flow cytometry assay demonstrated that PROX1-AS1 knockdown-induced cell apoptosis was abolished by miR-877-5p inhibitor, while knockdown of PD-L1 antagonized the impact of miR-877-5p inhibitor on the PROX1-AS1 knockdown cells (Figure 7D; $P < 0.01$). Besides, the transwell chamber assays manifested that the migration and invasion capacity of AGS and SGC7901 cells were suppressed by sh-PROX1-AS1, facilitated and retrieved by miR-877-5p inhibitors (Figure 7E; $P < 0.01$).

Discussion

As is known to all, many lncRNAs have been discovered due to the development of gene sequencing technology. In the last few years, the discovery of lncRNA which can be used as a prognostic marker provides a new light on the therapeutic targets of GC.[21–23] In our study, we firstly

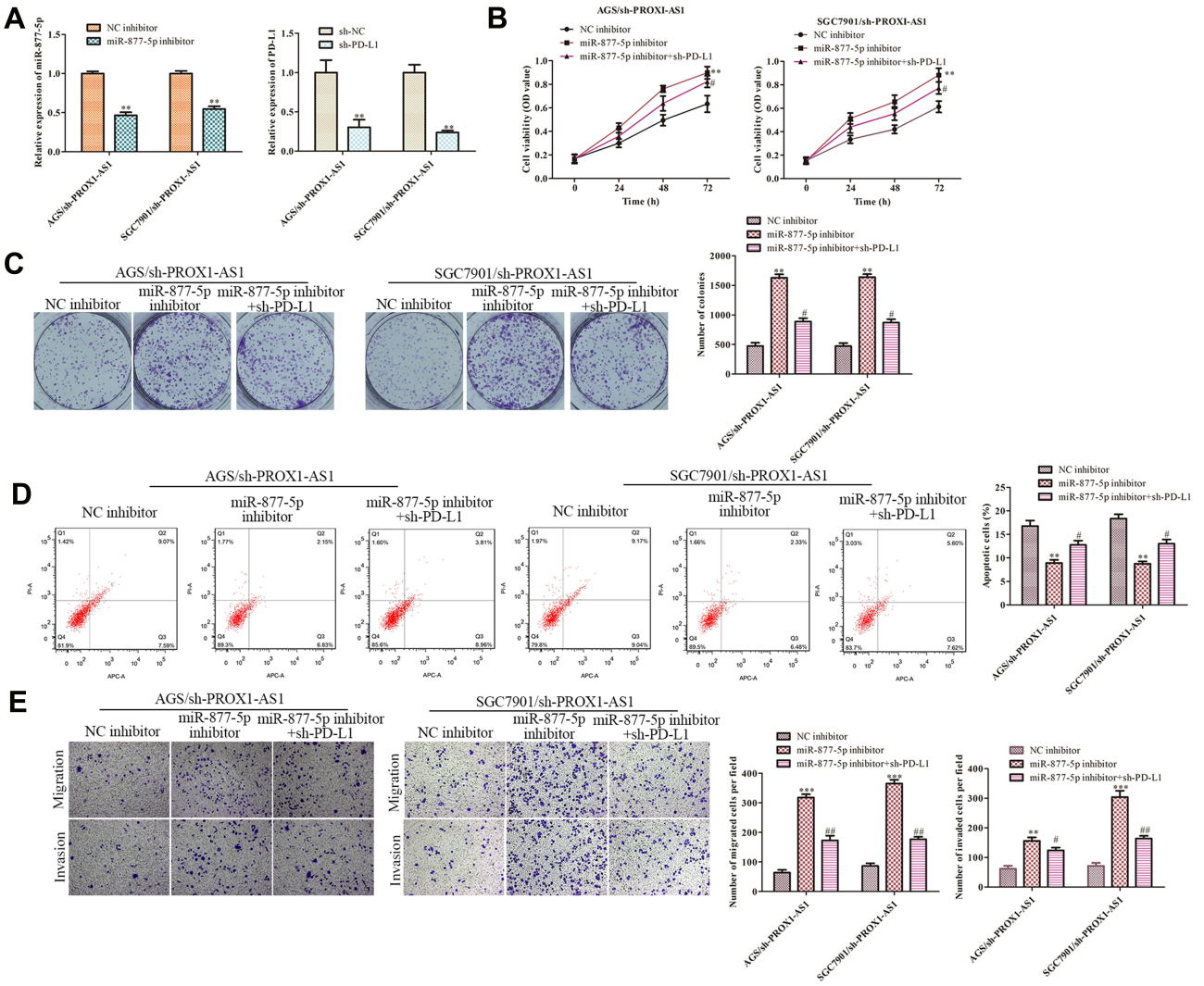

Figure 7 PROX1-AS1 promotes cell growth, invasion and inhibits apoptosis by targeting miR-877-5p/PD-L1 axis. (**A**) The RT-qPCR assay was implemented to certify transfection efficiency for miR-877-5p inhibitor and sh-PD-L1. (**B**–**E**) CCK-8, colony formation, flow cytometry, and transwell assays were employed to estimate the role of PROX1-AS1/miR-877-5p/PD-L1 axis in GC cell proliferation, migration, invasion and apoptosis. $^{**}P < 0.01$, $^{***}P < 0.001$ vs NC inhibitor group. $^{\#}P < 0.01$, $^{\#\#}P < 0.05$ vs miR-877-5p inhibitor group.

explored the expression pattern of PROX1-AS1 in GC and adjacent non-cancerous tissues. We found that PROX1-AS1 was extremely up-regulated in GC tissues. Likewise, previous studies have found that PROX1-AS1 is frequently induced in many cancer tissues. For example, lncRNA PROX1-AS1 is up-regulated and promotes proliferation in papillary thyroid carcinoma.[24] Furthermore, PROX1-AS1 has been proved to promote the GC proliferation and migration by activating FGFR1.[25] Additionally, PROX1-AS1 accelerates tumor progression by targeting miR-647 in GC.[26] Among them, PROX1-AS1 serves as an oncogene in GC progression.

To probe the biological effect and mechanism of PROX1-AS1 in the progression of GC, we performed loss-of-function tests. The results indicated that down-regulation of PROX1-AS1 impeded the proliferation and migration, invasion, while accelerating apoptosis of GC cells, indicating that PROX1-AS1 was an oncogene in GC. Furthermore, we confirmed that miR-877-5p was a potential target of PROX1-AS1 on the basis of bioinformatic analysis. Afterwards, the dual luciferase report assay was performed to validate the predication, and we found that miR-877-5p mimic inhibited the activity of luciferase reporter fused with WT PROX1-AS1 3′ UTR, but not fused with MUT PROX1-AS1 3′ UTR. By using qRT-PCR, we discovered that the miR-877-5p expression level was low expressed in GC tissues and cell lines, and negatively correlated with the expression of PROX1-AS1.

It is well established that miRNAs regulate the biological effects of cancer cells' function binding to the mRNA 3′ UTR and thereby negatively regulating mRNA expression.[3,27–30] Research proves that miR-877-5p suppresses bladder cancer cell proliferation by up-regulating p16.[31] Additionally, miR-877-3p is related to myofibroblast differentiation and lung fibrosis by targeting Smad7.[32] According to the inhibition role of miR-877-5p on tumor progression previously reported, we explored the effect of miR-877-5p on GC progression. Results of the present study suggested that ectopic of miR-877-5p expression suppressed the cell proliferation, invasion and induced cell apoptosis of GC. More importantly, we demonstrated that PD-L1 serving as a direct target of miR-877-5p was negatively regulated. A series of experiments illustrated that miR-877-5p directly correlated with PD-L1. Mechanistically, as evidenced by rescue experiment, we demonstrated that PROX1-AS1 knockdown induced reduction in cell proliferation, and invasion ability was promoted by the miR-877-5p inhibitor, while the effect of miR-877-5p inhibitor was subsequently recovered by PD-L1 depletion.

Taken together, these results indicated that knockdown of PROX1-AS1 suppressed the proliferation and migration, while enhancing the apoptosis of GC cells via miR-877-5p/PD-L1 axis. In short, our study provided a novel target for the diagnosis and treatment for GC patients.

Data Sharing Statement

All data generated or analyzed during this study are included in this published article.

Acknowledgments

We deeply appreciate the supports by all participants.

Funding

Changshu Municipal Health and Family Planning Commission Science and Technology Plan Youth Project (No. cswsq201809) and Suzhou science and technology development plan project (Livelihood Science and technology-Basic Research on medical and health application) (No: SYSD2018020).

Disclosure

The authors state that there is no conflict of interest.

References

1. Gong C, Hu Y, Zhou M, et al. Identification of specific modules and hub genes associated with the progression of gastric cancer. *Carcinogenesis*. 2019;40(10):1269–1277. doi:10.1093/carcin/bgz040
2. Tan HY, Wang C, Liu G, et al. Long noncoding RNA NEAT1-modulated miR-506 regulates gastric cancer development through targeting STAT3. *J Cell Biochem*. 2019;120(4):4827–4836. doi:10.1002/jcb.26691
3. Gu C, Zhang M, Sun W, Dong C. Upregulation of miR-324-5p inhibits proliferation and invasion of colorectal cancer cells by targeting ELAVL1. *Oncol Res*. 2019;27(5):515–524. doi:10.3727/096504018X15166183598572
4. Liu T, Liu S, Xu Y, et al. Circular RNA-ZFR inhibited cell proliferation and promoted apoptosis in gastric cancer by sponging miR-130a/miR-107 and modulating PTEN. *Cancer Res Treat*. 2018;50(4):1396–1417. doi:10.4143/crt.2017.537
5. Dong C, Sun J, Ma S, et al. K-ras-ERK1/2 down-regulates H2A.X (Y142ph) through WSTF to promote the progress of gastric cancer. *BMC Cancer*. 2019;19(1):530. doi:10.1186/s12885-019-5750-x
6. Song Y, Tong C, Wang Y, et al. Effective and persistent antitumor activity of HER2-directed CAR-T cells against gastric cancer cells in vitro and xenotransplanted tumors in vivo. *Protein Cell*. 2018;9(10):867–878. doi:10.1007/s13238-017-0384-8
7. Zhu C, Huang Q, Zhu H. Melatonin inhibits the proliferation of gastric cancer cells through regulating the miR-16-5p-Smad3 pathway. *DNA Cell Biol*. 2018;37(3):244–252. doi:10.1089/dna.2017.4040
8. Datta J, Da Silva EM, Kandoth C, et al. Poor survival after resection of early gastric cancer: extremes of survivorship analysis reveal distinct genomic profile. *Br J Surg*. 2020;107(1):14–19. doi:10.1002/bjs.11443
9. Lei K, Liang X, Gao Y, et al. Lnc-ATB contributes to gastric cancer growth through a MiR-141-3p/TGFβ2 feedback loop. *Biochem Biophys Res Commun*. 2017;484(3):514–521. doi:10.1016/j.bbrc.2017.01.094
10. Zhong F, Zhang W, Cao Y, et al. LncRNA NEAT1 promotes colorectal cancer cell proliferation and migration via regulating glial cell-derived neurotrophic factor by sponging miR-196a-5p. *Acta Biochim Biophys Sin*. 2018;50(12):1190–1199. doi:10.1093/abbs/gmy130
11. Guo H, Yang S, Li S, et al. LncRNA SNHG20 promotes cell proliferation and invasion via miR-140-5p-ADAM10 axis in cervical cancer. *Biomed Pharmacother*. 2018;102:749–757. doi:10.1016/j.biopha.2018.03.024
12. Jing N, Huang T, Guo H, et al. LncRNA CASC15 promotes colon cancer cell proliferation and metastasis by regulating the miR-4310/LGR5/Wnt/β-catenin signaling pathway. *Mol Med Rep*. 2018;18(2):2269–2276. doi:10.3892/mmr.2018.9191
13. Zhao J, Du P, Cui P, et al. LncRNA PVT1 promotes angiogenesis via activating the STAT3/VEGFA axis in gastric cancer. *Oncogene*. 2018;37(30):4094–4109. doi:10.1038/s41388-018-0250-z
14. Qin Y, Sun W, Zhang H, et al. LncRNA GAS8-AS1 inhibits cell proliferation through ATG5-mediated autophagy in papillary thyroid cancer. *Endocrine*. 2018;59(3):555–564. doi:10.1007/s12020-017-1520-1
15. Yan Q, Tian Y, Hao F. Downregulation of lncRNA UCA1 inhibits proliferation and invasion of cervical cancer cells through miR-206 expression. *Oncol Res*. 2018. doi:10.3727/096504018X15185714083446
16. Yan TH, Qiu C, Sun J, et al. MiR-877-5p suppresses cell growth, migration and invasion by targeting cyclin dependent kinase 14 and predicts prognosis in hepatocellular carcinoma. *Eur Rev Med Pharmacol Sci*. 2018;22(10):3038–3046. doi:10.26355/eurrev_201805_15061
17. Wu K, Yu Z, Tang Z, et al. miR-877-5p suppresses gastric cancer cell proliferation through targeting FOXM1. *Onco Targets Ther*. 2020;13:4731–4742. doi:10.2147/OTT.S251916

18. Pafundi PC, Caturano A, Franci G. Comment on: miR-877-5p suppresses cell growth, migration and invasion by targeting cyclin dependent kinase 14 and predicts prognosis in hepatocellular carcinoma. *Eur Rev Med Pharmacol Sci*. 2018;22(14):4401–4402. doi:10.26355/eurrev_201807_15489
19. Gu L, Chen M, Guo D, et al. PD-L1 and gastric cancer prognosis: a systematic review and meta-analysis. *PLoS One*. 2017;12(8): e0182692. doi:10.1371/journal.pone.0182692
20. Zhang C, Li Z, Xu L, et al. CXCL9/10/11, a regulator of PD-L1 expression in gastric cancer. *BMC Cancer*. 2018;18(1):462. doi:10.1186/s12885-018-4384-8
21. Lv XB, Lian G-Y, Wang H-R, et al. Long noncoding RNA HOTAIR is a prognostic marker for esophageal squamous cell carcinoma progression and survival. *PLoS One*. 2013;8(5):e63516. doi:10.1371/journal.pone.0063516
22. Liu XH, Sun M, Nie FQ, et al. Lnc RNA HOTAIR functions as a competing endogenous RNA to regulate HER2 expression by sponging miR-331-3p in gastric cancer. *Mol Cancer*. 2014;13:92. doi:10.1186/1476-4598-13-92
23. Zhao W, Geng D, Li S, et al. LncRNA HOTAIR influences cell growth, migration, invasion, and apoptosis via the miR-20a-5p/HMGA2 axis in breast cancer. *Cancer Med*. 2018;7(3):842–855. doi:10.1002/cam4.1353
24. Yanyan S, Erjie X, Adheesh B. LncRNA PROX1-AS1 promotes proliferation, invasion, and migration in Papillary thyroid carcinoma[J]. *Biosci Rep*. 2018;BSR20180862.
25. Jiang W, Meng K. Long non-coding RNA PROX1-AS1 promotes the proliferation and migration in gastric cancer by epigenetically activating FGFR1. *Panminerva Med*. 2019;29.
26. Song X, Bi Y, Guo W. Long noncoding RNA PROX1-AS1 promotes tumor progression and aggressiveness by sponging miR-647 in gastric cancer. *Minerva Med*. 2019;11. doi:10.23736/S0026-4806.19.06223-2
27. Wang F, Shan S, Huo Y, et al. MiR-155-5p inhibits PDK1 and promotes autophagy via the mTOR pathway in cervical cancer. *Int J Biochem Cell Biol*. 2018;99:91–99. doi:10.1016/j.biocel.2018.04.005
28. Li X, Yang H, Yang T. T.J.O.r. Yang, miR-122 inhibits hepatocarcinoma cell progression by targeting LMNB2. *Oncol Res*. 2020;28(1):41–49. doi:10.3727/096504019X15615433287579
29. Guan C, Yang C, Wang Y, et al. Comment on 'miR-338-5p inhibits cell proliferation, colony formation, migration, and cisplatin resistance in esophageal squamous cancer cells by targeting FERMT2'. *Carcinogenesis*. 2020;41(2):246. doi:10.1093/carcin/bgz089
30. Zhao L, Zhang Y, Liu J, et al. miR-185 inhibits the proliferation and invasion of non-small cell lung cancer by targeting KLF7. *Oncol Res*. 2019;27(9):1015–1023. doi:10.3727/096504018X15247341491655
31. Li S, Zhu Y, Liang Z, et al. Up-regulation of p16 by miR-877-3p inhibits proliferation of bladder cancer. *Oncotarget*. 2016;7(32):51773–51783. doi:10.18632/oncotarget.10575
32. Wang C, Gu S, Cao H, et al. miR-877-3p targets Smad7 and is associated with myofibroblast differentiation and bleomycin-induced lung fibrosis. *Sci Rep*. 2016;6:30122. doi:10.1038/srep30122